MORPHOLOGIES, OPTICAL AND ELECTRICAL CHARACTERIZATION OF ALUMINUM TIN SULFIDE THIN FILM.

MUHAMAD FAIZ BIN HASHIM

UNIVERSITI TEKNOLOGI MALAYSIA

MORPHOLOGIES, OPTICAL AND ELECTRICAL CHARACTERIZATION OF ALUMINUM TIN SULFIDE THIN FILM

MUHAMAD FAIZ BIN HASHIM

A thesis submitted in fulfillment of the
requirements for the award of the degree of
Master of Philosophy

Faculty of Science
Universiti Teknologi Malaysia

AUGUST 2017

I dedicate this work

To my beloved and lovely mother and late-father,
Mrs Habibah Bte A.Kadir
Mr Hashim Bin Samin
For the love, kindness, patience and prayer that have brought me to this far.

To my family and siblings,
Nur Nadia Hanim Bte Hashim and Muhamad Faisal Bin Hashim
For their love, understanding and support.

Special thanks to my supervisors and co-supervisor
Dr Wan Nurulhuda Bte Wan Shamsuri & Dr Rashid Ahmed
For all their kindness, help and prayers.

A thousand thanks to all lecturers for their help and advices.

To all my friends
For their endless laughs and tears....

ACKNOWLEDGEMENT

First of all, I would like to thank to Allah S.W.T most Gracious and most Merciful.

I wished to express my sincere appreciation to my supervisor, Dr Wan Nurulhuda Bte Wan Shamsuri and my co-supervisor Dr Rashid Ahmed who always giving help, guidance and encouragement throughout the process of completing my project. I would like to take this opportunity also to thank to all lecturers who helped me in planning, conducting and finishing this project.

I want to express gratitude to my beloved mother, Mrs Habibah Bte A.Kadir for always be my supporter, give encouragement and sacrificed time and money throughout these years. A special thanks to Universiti Teknologi Malaysia and Universiti Tun Hussien Onn Malaysia for giving the facilities for my project. I would like to thank to all laboratory assistants and technicians for their technical advised and support during the experimental works.

My appreciation also goes to everybody that involved directly or indirectly in helping me completing this thesis. Lastly, I would like to express my gratitude for the support of the sponsors with Project No Q.J130000.2526.10H77 and to Ministry of Education Malaysia (MoE) for funding my master study via MyBrain15-MyMaster scholarship program.

Praise to ALLAH S.W.T for His help and guidance that I finally able to complete this thesis.

ABSTRACT

Tin (II) sulfide (SnS) has caught many researcher's attentions as alternative material for solar cell absorber layer due to its abundance in nature, high absorption coefficient ($\alpha > 10^4$ cm^{-1}) and ideal energy bandgap (in the range of 1.3 – 1.5 eV) that make SnS a suitable candidate for solar cell absorber layer. Aluminum doped SnS (Al:SnS) thin films were deposited onto glass substrates using thermal evaporator machine and annealed at 200^{o}C for 2 hours under vacuum environment. The effects of doping at different weight percentages and annealing processes were investigated thoroughly using X-Ray diffraction (XRD) unit, scanning electron microscope (SEM), atomic force microscope (AFM) and ultra-violet visible (UV-Vis) spectrophotometer. From the XRD pattern, it was confirmed that Al:SnS thin films were successfully deposited using thermal evaporation technique. All the thin film samples were polycrystalline SnS oriented along the (111) direction with orthorhombic structure. XRD results also showed that doping and annealing processes increased the crystallite size of the thin film samples. Based on the SEM and AFM data, uniform thin film surfaces were obtained from samples that underwent the annealing process. UV-Vis spectral analysis indicated that the energy bandgaps for all samples were in the range of 1.32 to 1.49 eV, which were suitable for solar cell applications. From the four point probe measurement, it was found that SnS samples with lower resistivity were achieved when the samples were doped with aluminum. As conclusion, doping percentage and annealing process play vital role in producing high quality and suitable Al:SnS thin films for solar cell absorber layer.

ABSTRAK

Stanum (II) sulfida (SnS) telah menarik perhatian ramai penyelidik sebagai bahan alternatif bagi lapisan penyerap sel solar kerana lambakan semulajadinya, pekali penyerapannya yang tinggi ($\alpha > 10^4$ cm^{-1}) dan juga jurang tenaganya yang ideal (dalam julat 1.3-1.5 eV) yang menjadikannya calon yang sesuai sebagai lapisan penyerap sel solar. Saput tipis SnS berdop aluminium (Al:SnS) telah diendapkan pada substrat kaca menggunakan mesin penyejat haba dan disepuhlindapkan pada suhu 200^{o}C selama 2 jam dalam persekitaran bervakum. Kesan dopan dengan peratusan berat berbeza dan proses penyepuhlindapan telah dikaji secara menyeluruh menggunakan unit pembelauan sinar-X (XRD), mikroskop elektron pengimbas (SEM), mikroskop daya atom (AFM) dan spektrofotometer ultra lembayung-boleh nampak (UV-Vis). Daripada corak XRD, disahkan bahawa saput tipis Al:SnS telah berjaya diendap menggunakan teknik penyejatan haba. Kesemua sampel saput tipis adalah polihablur SnS berorentasi sepanjang arah (111) dengan struktur ortorombik. Keputusan XRD turut menunjukkan bahawa proses dopan dan penyepuhlindapan telah meningkatkan saiz kristal sampel saput tipis. Berdasarkan data SEM dan AFM, permukaan saput tipis yang seragam diperolehi daripada sampel yang telah menjalani proses penyepuhlindapan. Analisis spektrum UV-Vis menunjukkan bahawa jurang tenaga semua sampel berada dalam julat 1.32 hingga 1.49 eV. Daripada pengukuran prob empat titik, didapati sampel SnS dengan kerintangan yang lebih rendah telah diperolehi apabila sampel didopkan dengan aluminium. Sebagai kesimpulan, peratusan dopan dan proses penyepuhlindapan memainkan peranan penting dalam menghasilkan saput tipis Al:SnS yang berkualiti tinggi dan sesuai untuk dijadikan lapisan penyerap sel solar.

TABLE OF CONTENTS

LIST OF TABLES

LIST OF FIGURES

LIST OF ABBREVIATIONS & SYMBOLS

AFM	-	Atomic force microscope
Ag	-	Silver
Al:SnS	-	Aluminum doped tin (II) sulphide
Bi	-	Bismuth
Al	-	Aluminum
BSE	-	Back scattering electron
CdTe	-	Cadmium telluride
CIGS	-	Copper indium gallium diselenide
Cu	-	Copper
DTA	-	Deferential thermal analysis
EDX	-	Energy dispersive X-ray
H_2S	-	Hydrogen sulphide
IBM	-	International business machines corporation
JCPDS	-	Joint Committee on Powder Diffraction Standards
NREL	-	National Renewable Energy Laboratory
PV	-	Photovoltaic
S	-	Sulphur
Sb	-	Antimony
SEM	-	Scanning electron meter
Sn	-	Tin
$SnCl_2$	-	Tin (II) Chloride
SnS	-	Tin (II) sulphide
UV-Vis Spectroscopy	-	Ultraviolet-visible spectroscopy
wt%	-	Weight percentage
XRD	-	X-ray diffraction
λ	-	Wavelength
θ	-	Angle
π-electrons	-	Bonding electron
n-electrons	-	Non-bonding electron
A	-	Absorbance
α		absorption coefficient
$h\nu$	-	Photon energy

E_g	-	Energy bandgap
I	-	Current
V	-	Voltage
ρ	-	Resistivity
R_s	-	Sheet resistance

LIST OF APPENDICES

CHAPTER 1

INTRODUCTION

1.1 Introduction

In this chapter, the general information that is related to this project would be presented and discussed. This research was done to investigate the effect of aluminum (Al) doping and annealing process towards the changes of tin (II) sulfide thin film properties. This chapter consists of the background of study, problem of statement, objectives of study, scope of study and significance of study for this research.

1.2 Background of Study

Cadmium telluride (CdTe) or copper indium gallium diselenide (Cu (In,Ga)Se_2 or CIGS) based absorber layer are the most advanced and promising materials that are used for solar cell applications, due to its high conversion efficiencies of solar energy into electricity (Barkhouse *et al.*, 2012; Meyers, 1988; Paudel *et al.*, 2012; Pawar *et al.*, 2014). However, these two materials are considered as very rare materials in nature, and it is harder for mass scale solar cell production in the near future. Besides that, cadmium based material are also classified as toxic material and banned in several Europe country (Aberle., 2009; Henry *et al.*, 2013; Ramakrishna Reddy *et al.*, 2006). This has encouraged researchers to find alternative materials for absorber layer in thin film solar cell application. One of the most promising material candidates for thin film solar cell is tin (II) sulfide (SnS). This is due to, it have direct energy band gap in the range of 1.2–1.5 eV and high absorption coefficient ($\alpha > 10^4$ cm^{-1}) (Miles *et al.*, 2009; Nwofe *et al.*, 2012; Schneikart *et al.*, 2013; Zhang *et al.*, 2011). Furthermore, tin and sulfur are considered as non-toxic material and abundant in nature. It is theoretically estimated that the conversion efficiency for tin (II) sulfide thin film solar cell is more than 24% (Zhang *et al.*, 2011).

The properties of tin (II) sulfide thin film can be easily controlled by doping with a suitable metallic material, such as silver (Ag) (Devika *et al.*, 2006), bismuth (Bi) (Manohari *et al.*, 2011), antimony (Sb) (Sinsermsuksakul, *et al.*, 2014) and copper (Cu) (Zhang & Cheng, 2011). Doping process help researcher to obtain a much higher absorption coefficient and less resistivity tin (II) sulfide thin film for solar cell application. Post annealing process also plays vital role for producing high quality thin film, by structural recrystallization, grain size growth and abate the surface morphology. In this study, investigation on the characteristics of the aluminum doped tin (II) sulfide (Al: SnS) thin film are done. The influence of Al doping concentration and the effect of post annealing process toward the thin film samples were analyzed thoroughly.

A solar cell is an electrical device that converts solar energy into electrical energy. Solar cell is an off-grid device that is able to generate electricity without any external voltage source. Solar cell has been discovered since the year 1839 by French physicist Edmond Becquerel (Fraas, 2014). Since then, solar cell has undergone a lot of improvements and development. This is due to the growth of understanding the true cost of fossil fuels and with the widespread demand for renewable and environmentally acceptable energy resources. Nowadays solar cell has been used widely in many fields. Solar cell has been installed in home and it also has been used by NASA to power up their space station and robots in the outer space. Solar cell has enabled human to do a lot of things and discovers things beyond this world.

1.3 Problem of Statement

Recent investigation in photovoltaic studies are more focusing on finding new absorber materials for replacing cadmium (Cd), arsenic (As), selenium (Se) and silicon (Si) based material with less toxicity, abundant in nature, cost efficient and have comparable energy conversion efficiencies (Reddy *et al.*, 2006) . In this direction, tin (II) sulfide (SnS) based material has caught many researcher attention as a potential absorber layer. With its high absorption coefficient ($\alpha > 10^4$ cm^{-1}) and near optimum direct energy band gap for solar cell application (E_g~ 1.4 eV) making it a suitable candidate as an absorber layer for photovoltaic cell (Tariq *et al*., 2014; Miles *et al.*, 2009; Nwofe *et al.*, 2012).

However, with its high resistivity and low conductivity compared to others absorber materials such as cadmium telluride (CdTe) and copper indium gallium selenide (CIGS), new approach is needed to overcome this problem. By introducing dopant materials to SnS, is considered as the best option. It has been reported that SnS are being doped with antimony (Sb), copper (Cu) and bismuth (Bi) to improve their electrical and optical properties (Manohari *et al.*, 2011; Sinsermsuksakul *et al.*, 2014; Zhang & Cheng, 2011).

One of the suitable dopant materials for SnS is aluminum (Al). Based on the study reported by Zhang *et al.*, they stated that Al as dopant materials (5 wt% to 15 wt%) has decreased the resistivity from 650 to 4.55 **Ω**·cm, and improve the optical properties of the SnS thin films. Nonetheless, the effect of high doping concentration and post annealing process were not yet been reported. Hence, higher Al doping concentration and annealed thin film samples are produced for this study.

1.4 Objectives of Study

The objectives of this study are:

i. To fabricate undoped and aluminum doped tin (II) sulfide thin film at different doping weight percentage (0, 5, 10, 15 and 20 wt%) by using thermal evaporation method and then annealing at 200^0C for 2 hours in vacuum environment using tube furnace.
ii. To examine the structural characteristic of undoped and aluminum doped tin (II) sulfide thin film.
iii. To determine the optical characteristic of undoped and aluminum doped tin (II) sulfide thin film.
iv. To investigate the electrical characteristic of undoped and aluminum doped tin (II) sulfide thin film.

1.5 Scope of Study

In sequence to achieve the given objectives, the works had been focused on the following tasks.

i. Thermal evaporation technique was utilized to fabricate undoped and aluminum doped tin (II) sulfide thin film samples with different doping weight percentage.
ii. All thin film samples were annealed for 2 hours in vacuum environment using tube furnace.
iii. The structure and crystal phase of undoped and aluminum doped tin (II) sulfide thin films were identified using X-Ray diffraction (XRD) instrument.
iv. The surface morphology of the undoped and aluminum doped tin (II) sulfide thin film samples were studied using scanning electron microscope (SEM) and atomic force microscope (AFM).
v. UV-Vis Spectrophotometer was used to explore the optical properties of undoped and aluminum doped tin (II) sulfide thin film.
vi. The electrical characteristic of undoped and aluminum doped tin (II) sulfide thin film such as resistivity and conductivity were investigated by utilize four point probe technique.

1.6 Significance of Study

This study may help other researchers to understand the effect of doping concentration and post annealing process towards the structural, optical and electrical characteristics of undoped and aluminum doped tin (II) sulfide thin film samples. The data obtained from this research are vital for gaining new knowledge and identify the changes of resistivity, conductivity, surface morphology, absorption coefficient and energy band gap when tin (II) sulfide thin film are doped with aluminum dopant and undergoes post annealing process.

REFERENCES

Abed, R. A., and Habeeb, M. A. (2013). Preparation and Study Optical Properties of (PVA-PVP-$CrCl_2$) Composites, *Industrial Engineering Letters*. *3*(7), 606–610.

Aberle, A. G. (2009). Thin-film solar cells. *Thin Solid Films*, *517*(17), 4706–4710.

Adachi, H., and Wasa, K. (2012). Thin Films and Nanomaterials. *Handbook of Sputter Deposition Technology: Fundamentals and Applications for Functional Thin Films*, Nano-Materials and MEMS, 1.

Akkari, A., Guasch, C., and Kamoun-Turki, N. (2010). Chemically deposited tin sulphide. *Journal of Alloys and Compounds*, *490*(1–2), 180–183.

Al-Kuhaili, M. F., Alade, I. O., and Durrani, S. M. A. (2014). Optical constants of hydrogenated zinc oxide thin films. *Optical Materials Express*, *4*(11), 2323-2331.

Alonzo-Medina, G. M., González-González, a, Sacedón, J. L., and Oliva, a I. (2013). Understanding the thermal annealing process on metallic thin films. *IOP Conference Series: Materials Science and Engineering*, *45(1), 012013*.

An, V., Dronova, M., and Zakharov, A. (2015). Optical and AFM studies on p-SnS thin films deposited by magnetron sputtering. *Chalcogenide Letters 12*(9), 483–487.

Bach, H., and Krause, D. (Eds.) (2003). *Thin films on glass*. Mainz, Germany. Springer Science & Business Media.

Bagher, A. M., Mahmoud, M., Vahid, A., and Mohsen, M. (2015). Types of Solar Cells and Application, *American Journal of Optics and Photonics*, *3*(5), 94–113.

Barkhouse, D. A. R., Gunawan, O., Gokmen, T., Todorov, T. K., and Mitzi, D. B. (2012). Device characteristics of a 10.1% hydrazine-processed $Cu_2ZnSn(Se,S)_4$ solar cell. *Progress in Photovoltaics: Research and Applications*, 20(1), 6–11.

Bashkirov, S. A., Gremenok, V. F., Ivanov, V. A., Lazenka, V. V., and Bente, K. (2012). Tin sulfide thin films and Mo/p-SnS/n-CdS/ZnO heterojunctions for photovoltaic applications. *Thin Solid Films, 520*(17), 5807–5810.

Ben Ayadi, Z., Mahdhi, H., Djessas, K., Gauffier, J. L., El Mir, L., and Alaya, S. (2014). Sputtered Al-doped ZnO transparent conducting thin films suitable for silicon solar cells. *Thin Solid Films*, *553*, 123–126.

Binnig, G., and Quate, C. F. (1986). Atomic Force Microscope. *Physical Review Letters*, *56*(9), 930–933.

Burstein, E. (1954). Anomalous Optical Absorption Limit in InSb. *Physical Review*, *93*(3), 632–633.

Burton, L. A, and Walsh, A. (2012). Phase Stability of the Earth-Abundant Tin Sulfides SnS, SnS_2 and Sn_2S_3. *The Journal of Physical Chemistry C*, 116(45), 24262-24267.

Butt, H. J., Cappella, B., and Kappl, M. (2005). Force measurements with the atomic force microscope: Technique, interpretation and applications. *Surface Science Reports*, *59*(1–6), 1–152.

Calixto-Rodriguez, M., Martinez, H., Sanchez-Juarez, a., Campos-Alvarez, J., Tiburcio-Silver, a., & Calixto, M. E. (2009). Structural, optical, and electrical properties of tin sulfide thin films grown by spray pyrolysis. *Thin Solid Films*, *517*(7), 2497–2499.

Cha, J. H., Ashok, K., Kissinger, N. S., Ra, Y. H., Sim, J. K., Kim, J. S., and Lee, C. R. (2011). Effect of thermal annealing on the structure, morphology, and electrical properties of Mo bottom electrodes for solar cell applications. *Journal of the Korean Physical Society*, *59*(3), 2280-2285.

Chapin, D. M., Fuller, C. S., & Pearson, G. L. (1954). A New Silicon p-n Junction Photocell for Converting Solar Radiation into Electrical Power. *Journal of Applied Physics*, *25*(5), 676 -677.

Cheng, S., and Conibeer, G. (2011). Physical properties of very thin SnS films deposited by thermal evaporation. *Thin Solid Films*, *520*(2), 837–841.

Cifuentes, C., Botero, M., Romero, E., Calderón, C., & Gordillo, G. (2006). Optical and structural studies on SnS films grown by co-evaporation. *Brazilian Journal of Physics*, *36*(3b), 1046–1049.

D'Antò, V., Rongo, R., Ametrano, G., Spagnuolo, G., Manzo, P., Martina, R., and Valletta, R. (2012). Evaluation of surface roughness of orthodontic wires by means of atomic force microscopy. The Angle Orthodontist, 82(5), 922–928.

Dabagh, S. Y. Al, and Makhool, E. E. (2016). The Effect of Fe Concentration on the Structure and Optical Properties of Zno Films by Using Pulsed Laser Deposition. *Journal of Dental and Medical Sciences*, 15(2), 54–60.

Devika, M., Reddy, N. K., Ramesh, K., Gunasekhar, K. R., Gopal, E. S. R., and Ramakrishna Reddy, K. T. (2006). Low resistive micrometer-thick SnS:Ag films for optoelectronic applications. *Journal of the Electrochemical Society*, *153*(8), G727-G733.

Devika, M., Reddy, N. K., Ramesh, K., Ganesan, R., Gunasekhar, K. R., Gopal, E. S. R., and Reddy, K. R. (2007). Thickness effect on the physical properties of evaporated SnS films. *Journal of the Electrochemical Society*, 154(2), 1125–1131.

Devika, M., Reddy, N. K., Reddy, D. S., Ahsanulhaq, Q., Ramesh, K., Gopal, E. S. R., and Hahn, Y. B. (2008). Synthesis and characterization of nanocrystalline SnS films grown by thermal evaporation technique. *Journal of The Electrochemical Society*, 155(2), H130-H135.

Duffie, J. A., and Beckman, W. A. (2013). *Solar Engineering of Thermal Processes.* Hoboken, New Jersy. John Wiley & Sons.

Doherty, R. D., Hughes, D. A., Humphreys, F. J., Jonas, J. J., Juul Jensen, D., Kassner, M. E., and Rollett, A. D. (1998). Current issues in recrystallization: A review. *Materials Today*, *1*(2), 14–15.

Ewald, P. P., and Barlow, M. (1963). Fifty Years of X-Ray Diffraction. *Physics Today*, *16*, 70.

Fraas, L. M. (2014). *History of Solar Cell Development. "Low-Cost Solar Electric Power".* Bellevue, Washington. Springer International Publishing.

Ghosh, B., Bhattacharjee, R., Banerjee, P., and Das, S. (2011). Structural and optoelectronic properties of vacuum evaporated SnS thin films annealed in argon ambient. *Applied Surface Science*, *257*(8), 3670–3676.

Goetzberger, A., Hebling, C., and Schock, H. W. (2003). Photovoltaic materials, history, status and outlook. *Materials Science and Engineering: R: Reports*, *40*(1), 1-46.

Gordillo, G., Botero, M., and Oyola, J. S. (2008). Synthesis and study of optical and structural properties of thin films based on new photovoltaic materials. *Microelectronics Journal*, *39*(11), 1351–1353.

Goswami, A. (1996). *Thin Film Fundamentals*. New Delhi, India. New Age International.

Green, M. A., Emery, K., Hishikawa, Y., Warta, W., and Dunlop, E. D. (2015). Solar cell efficiency tables (Version 45). *Progress in Photovoltaics: Research and Applications*, *23*(1), 1–9.

Grundmann, M. (2015). *The physics of semiconductors: an introduction including nanophysics and applications.* Leipzig, Germany. Springer.

Haque, M. A., and Mahalakshmi, S. (2014). Effect of annealing on structure and morphology of cadmium sulphide thin film prepared by chemical bath deposition. *Journal of Advanced Physics*, *3*(2), 159–162.

Hartman, K., Johnson, J. L., Bertoni, M. I., Recht, D., Aziz, M. J., Scarpulla, M. A., and Buonassisi, T. (2011). SnS thin-films by RF sputtering at room temperature. *Thin Solid Films*, *519*(21), 7421-7424.

Henry, J., Mohanraj, K., Kannan, S., Barathan, S., and Sivakumar, G. (2015). Structural and optical properties of SnS nanoparticles and electron-beam-evaporated SnS thin films. *Journal of Experimental Nanoscience, 10*(2), 78-85.

Indirajith, R., Srinivasan, T. P., Ramamurthi, K., and Gopalakrishnan, R. (2010). Synthesis, deposition and characterization of tin selenide thin films by thermal evaporation technique. *Current Applied Physics*, 10(6), 1402–1406.

Kafashan, H., Ebrahimi-Kahrizsangi, R., Jamali-Sheini, F., and Yousefi, R. (2016). Effect of Al doping on the structural and optical properties of electrodeposited SnS thin films. *Physica Status Solidi (a)*, 213(5), 1302–1308.

Koteeswara Reddy, N., Hahn, Y. B., Devika, M., Sumana, H. R., and Gunasekhar, K. R. (2007). Temperature-dependent structural and optical properties of SnS films. *Journal of Applied Physics*, 101(2007), 4–11.

Lu, X. M., Zhu, J. S., Zhang, W. Y., Ma, G. Q., and Wang, Y. N. (1996). The energy gap of r.f.-sputtered BaTiO3 thin films with different grain size. *Thin Solid Films*, 274(1–2), 165–168.

Majumder, S. ., Jain, M., and Katiyar, R. . (2002). Investigations on the optical properties of sol–gel derived lanthanum doped lead titanate thin films. *Thin Solid Films*, 402(1), 90–98.

Manjula, N., Pugalenthi, M., Nagarethinam, V. S., Usharani, K., and Balu, A. R. (2015). Effect of doping concentration on the structural, morphological, optical and electrical properties of Mn-doped CdO thin films. *Materials Science-Poland*, *33*(4), 774–781.

Manohari, A. G., Dhanapandian, S., Manoharan, C., Kumar, K. S., and Mahalingam, T. (2011). Effect of doping concentration on the properties of bismuth doped tin sulfide thin films prepared by spray pyrolysis. *Ceramics International*, 37(2), 555–560.

Mathews, N. R., Colín García, C., and Torres, I. Z. (2013). Effect of annealing on structural, optical and electrical properties of pulse electrodeposited tin sulfide films. *Materials Science in Semiconductor Processing,* 16(1), 29–37.

Meyers, P. V. (1988). Design of a thin film CdTe solar cell. Solar Cells, 23(1–2), 59–67.

Miles, R. W., Ogah, O. E., Zoppi, G., and Forbes, I. (2009). Thermally evaporated thin films of SnS for application in solar cell devices. *Thin Solid Films*, 517(17), 4702–4705.

Minnam Reddy, V. R., Gedi, S., Park, C., R.W, M., and K.T, R. R. (2015). Development of sulphurized SnS thin film solar cells. *Current Applied Physics*, 15(5), 588–598.

Noguchi, H., Setiyadi, A., Tanamura, H., Nagatomo, T., and Omoto, O. (1994). Characterization of vacuum-evaporated tin sulfide film for solar cell materials. *Solar energy materials and solar cells*, 35, 325-331.

Nadi, S. A., Chelvanathan, P., Zakaria, Z., Alam, M. M., Alothman, Z. A., Sopian, K., and Amin, N. (2014). Postdeposition Annealing Effect on Cu_2ZnSnS_4 Thin Films Grown at Different Substrate Temperature. *International Journal of Photoenergy*, 2014.

Nair, P. (1998). Semiconductor thin films by chemical bath deposition for solar energy related applications. *Solar Energy Materials and Solar Cells*, 52(3–4), 313–344.

Nwofe, P. a., Reddy, K. T. R., Tan, J. K., Forbes, I., and Miles, R. W. (2012). Thickness Dependent Optical Properties of Thermally Evaporated SnS Thin Films. *Physics Procedia*, 25, 150–157.

Nwofe, P. a, Reddy, K. T. R., Tan, J. K., Forbes, I., and Miles, R. W. (2013). On the Structural and Optical Properties of SnS Films Grown by Thermal Evaporation Method. *Journal of Physics: Conference Series*, 417 (1), 12039.

Ogah, O. E., Zoppi, G., Forbes, I., and Miles, R. W. (2009). Thin films of tin sulphide for use in thin film solar cell devices. *Thin Solid Films*, 517(7), 2485–2488.

Ortiz, a, Alonso, J. C., Garcia, M., and Toriz, J. (1999). Tin sulphide films deposited by plasma-enhanced chemical vapour deposition. *Semiconductor Science and Technology*, 11(2), 243–247.

Öztaş, M., Kaya, Z., and Öztaş, M. (2013). *Effect of boric acid content on the structural and optical properties of ZnO films prepared by spray pyrolysis technique*. International Conference on Energy, Regional Integration and Socio-economic Development. EcoMod.

Palchoudhury, S., Baalousha, M., and Lead, J. (2016). Methods for measuring concentration (mass, surface area and number) of nanoparticles. *Characterization of Nanomaterials in Complex Environmental and Biological Media, Eds Baalousha M, Lead J (Elsevier, Amsterdam)*, 153–177.

Paudel, N. R., Wieland, K. A., and Compaan, A. D. (2012). Ultrathin CdS/CdTe solar cells by sputtering. *Solar Energy Materials and Solar Cells*, 105, 109–112.

Pawar, S. M., Inamdar, A. I., Pawar, B. S., Gurav, K. V., Shin, S. W., Yanjun, X., and Im, H. (2014). Synthesis of Cu_2ZnSnS_4 (CZTS) absorber by rapid thermal processing (RTP) sulfurization of stacked metallic precursor films for solar cell applications. *Materials Letters*, 118, 76–79.

Perlin, J. (1999). *From Space to Earth: The Story of Solar Electricity*. Ann Arbor, Michigan. Aatec Publications.

Petrov, I., Barna, P. B., Hultman, L., and Greene, J. E. (2003). Microstructural evolution during film growth. *Journal of Vacuum Science & Technology A: Vacuum, Surfaces, and Films*, 21(5), S117-S128.

Ramakrishna Reddy, K. T., Koteswara Reddy, N., and Miles, R. W. (2006). Photovoltaic properties of SnS based solar cells. *Solar Energy Materials and Solar Cells*, 90(18–19), 3041–3046.

Ray, S. C., Karanjai, M. K., and Dasgupta, D. (1999). Structure and photoconductive properties of dip-deposited SnS and SnS_2 thin films and their conversion to tin dioxide by annealing in air. *Thin Solid Films*, 350(1), 72–78.

Reddy, N. K., and Reddy, K. T. R. (2005). SnS films for photovoltaic applications: Physical investigations on sprayed SnxSy films. *Physica B: Condensed Matter*, 368(1–4), 25–31.

Sader, J. E., Chon, J. W. M., and Mulvaney, P. (1999). Calibration of rectangular atomic force microscope cantilevers. *Review of Scientific Instruments*, 70(10), 3967–3969.

Salaken, S. M., Farzana, E., and Podder, J. (2013). Effect of Fe-doping on the structural and optical properties of ZnO thin films prepared by spray pyrolysis. *Journal of Semiconductors*, 34(7), 73003.

Santhosh Kumar, K., Manoharan, C., Dhanapandian, S., and Gowri Manohari, A. (2013). Effect of Sb dopant on the structural, optical and electrical properties of SnS thin films by spray pyrolysis technique. *Spectrochimica Acta Part A: Molecular and Biomolecular Spectroscopy*, 115, 840–844.

Schneikart, A, Schimper, H.-J., Klein, A, and Jaegermann, W. (2013). Efficiency limitations of thermally evaporated thin-film SnS solar cells. *Journal of Physics D: Applied Physics*, 46(30), 305109.

Schuetze, A. P., Lewis, W., Brown, C., and Geerts, W. J. (2004). A laboratory on the four-point probe technique. *American Journal of Physics*, *72*(2), 149-153.

Shehab, A. A., AL-Hamadni, N. A., and Latif, D. M. (2014). Effect of annealing temperature on structure properties of SnS thin films. *Physical Chemistry: An Indian Journal*, *9*(7), 255-259.

Sinsermsuksakul, P., Chakraborty, R., Kim, S. B., Heald, S. M., Buonassisi, T., and Gordon, R. G. (2012). Antimony-doped tin (II) sulfide thin films. *Chemistry of Materials*, *24*(23), 4556-4562.

Sinsermsuksakul, P., Sun, L., Lee, S. W., Park, H. H., Kim, S. B., Yang, C., and Gordon, R. G. (2014). Overcoming efficiency limitations of SnS-based solar cells. *Advanced Energy Materials*, *4*(15), 1–7.

Smeds, S. A. (1993). Herzenbergite (SnS) in Proterozoic Granite Pegmatites in North-Central Sweden. *Mineralogical Magazine*, 57(388), 489–494.

Smits, F. M. (1958). Measurement of sheet resistivities with the four-point probe. *Bell Labs Technical Journal*, *37*(3), 711-718.

Sze, S. M., and Ng, K. K. (2006). *Physics of semiconductor devices.* Hoboken, New Jersey. John Wiley & Sons.

Tanuševski, A., and Poelman, D. (2003). Optical and photoconductive properties of SnS thin films prepared by electron beam evaporation. *Solar Energy Materials and Solar Cells,* 80(3), 297–303.

Tariq, G. H., Hutchings, K., Asghar, G., Lane, D. W., and Anis-Ur-Rehman, M. (2014). Study of annealing effects on the physical properties of evaporated SnS thin films for photovoltaic applications. *Journal of Ovonic Research,* 10(6), 247–256.

Tauc, J. (1974). Amorphous and Liquid Semiconductors. *Optica Acta: International Journal of Optics,* 17(12), 952–952.

Tauc, J., and Abeles, F. (1972). *Optical properties of solids (Vol. 372).* North-Holland, Amsterdam. American Elsevier.

Thomas, N. C. (1991). The early history of spectroscopy. *Journal of Chemical Education,* 68(8), 631.

Tsay, C. Y., Cheng, H. C., Tung, Y. T., Tuan, W. H., and Lin, C. K. (2008). Effect of Sn-doped on microstructural and optical properties of ZnO thin films deposited by sol–gel method. *Thin Solid Films*, 517(3), 1032–1036.

Valdes, L. B. (1954). Measurement of sheet resistivities with the four point probe. *Procedings of the I.R.E.*, 29, 420–427.

Verly, P. G. (2013). *Optical Thin Films and Coatings. Optical Thin Films and Coatings*. Ottawa, Canada. Elsevier.

Vinodkumar, R., Navas, I., Chalana, S. R., Gopchandran, K. G., Ganesan, V., Philip, R., and Pillai, V. P. M. (2010). Applied Surface Science Highly conductive and transparent laser ablated nanostructured Al : ZnO thin films. *Applied Surface Science*, *257*(3), 708–716.

West, A. R. (2007). Solid state chemistry and its applications. Aberdeen, Scotland. John Wiley & Sons.

Yue, G. H., Wang, W., Wang, L. S., Wang, X., Yan, P. X., Chen, Y., and Peng, D. L. (2009). The effect of anneal temperature on physical properties of SnS films. *Journal of Alloys and Compounds*, 474, 445–449.

Yuying, G., Weimin, S., and Guangpu, W. (2008). Electrical Properties of Doped Sns Thin Films Prepared by Vacuum Evaporation. *In Proceedings of ISES World Congress 2007,* 1-5, 1337-1340.

Zhang, S., and Cheng, S. (2011). Thermally evaporated SnS: Cu thin films for solar cells. *IET Micro & Nano Letters*, *6*(7), 559-562.

Zhang, S., Cheng, S. Y., Jia, H. J., and Zhou, H. F. (2011). Preparation and Characterization of Aluminium-Doped SnS Thin Films. Advanced Materials Research, 418–420, 712–716.

Zhou, H., Yi, D., Yu, Z., Xiao, L., and Li, J. (2007). Preparation of aluminum doped zinc oxide films and the study of their microstructure, electrical and optical properties. *Thin Solid Films*, 515(17), 6909–6914.

Zhu, F. Y., Wang, Q.-Q., Zhang, X. S., Hu, W., Zhao, X., and Zhang, H. X. (2014). 3D nanostructure reconstruction based on the SEM imaging principle, and applications. *Nanotechnology*, 25(18), 185705.

APPENDIX A

Literature Review

Author (Year)	Experiment	Result
Reddy et al., (2006)	Material • Tin (II) sulfide. Deposition • Thermal evaporation.	XRD • The peak intensity (040) increased with the increase of the substrate temperature. EDAX • Existence of Sn and S elements. SEM • Grain size increased with the increase of the substrate temperature. UV-VIS Spectroscopy • Energy bandgap decrease when undergoes annealing process.
Yuying et al., (2007)	Material • Tin (II) Sulfide. • Sb, Sb2O3, Se, Te, In, In_2O_3, Se and In_2O_3. (Dopant) Deposition • Thermal evaporation.	Resistivity • Resistivity decrease as doping concentration increase (0.1 - 1.3 wt%) • Resistivity increase as doping concentration increase (1.3 – 2.5 wt%) Photocurrent and dark current • Value of G_{photo}/G_{dark} increase with increase of doping percentage. (0.1- 1.5 wt%). • Value of G_{photo}/G_{dark} decrease as doping concentration keep increase (1.5 – 12.5 wt%).

Author (Year)	Experiment	Result
Ogah et al., (2009)	Material • Tin (II) sulfide. Deposition • Thermal Evaporation.	XRD • The 3 predominant peaks for SnS are (111), (040) and (131). EDS • Substrate temperature increase, tin concentration decrease. • Source temperature increase, tin concentration increase. SEM • Pinhole free and densely packed columnar grains. UV-VIS Spectroscopy. • E_g for 300 °C = 1.45 eV, 350 °C = 1.65 eV (substrate temp)
Zhang et al., (2011)	Material • Tin (II) sulfide. • Aluminum. (Dopant) Deposition • Thermal Evaporation.	XRD • The intensity of SnS (111) increased with the increase of doping concentration. SEM • Grain density increase as Al doping increase. UV-VIS Spectroscopy • Energy band gap decreased with increased of doping concentration. (1.50eV – 1.29eV) Hall Effect • Decrease in resistivity with increasing Al concentration percentage. • P-type conductivity thin film (R_H positive)

Author (Year)	Experiment	Result
Zhang & Cheng, (2011)	Material • Tin (II) sulfide. • Copper. (Dopant) Deposition • Thermal Evaporation.	XRD • The 3 predominant peaks for SnS are the (111), (101) and (002). UV-VIS Spectroscopy • Energy band gap decrease as Cu doping concentration increase. Electrical Properties • Carrier concentration increases as doping concentration increased. • The resistivity decreases with the increase of doping concentration. • SnS:Cu exhibit p-type conductivity.
Ali et al., (2013)	Material • Tin, Sn • Antimony, Sb • Sulphur Deposition technique • Sputter coater.	EDS • Confirms the combinatorial deposition of SnSbS thin film. XRD • The existence of SnS, $Sn_2Sb_2S_5$, $SnSb_2S_4$, and $Sb_2Sn_5S_9$ phase. Photoconductivity • High annealing temperature, photoconductivity increases.
Lane et al.,(2014)	Material • Tin (II) sulfide. Deposition • Thermal Evaporation. Annealing Process. • Temp: 200°C, 300°C, 400°C. • Duration: 1 Hour.	XRD • Predominant peak for SnS is (111). • Peak intensity increase as annealing temperature increase. UV-VIS Spectroscopy. • Absorption coefficient increase, with annealing temp. • Optical bandgap, E_g range from 1.78 eV – 1.90 eV.

APPENDIX B

Correction Factor Graph

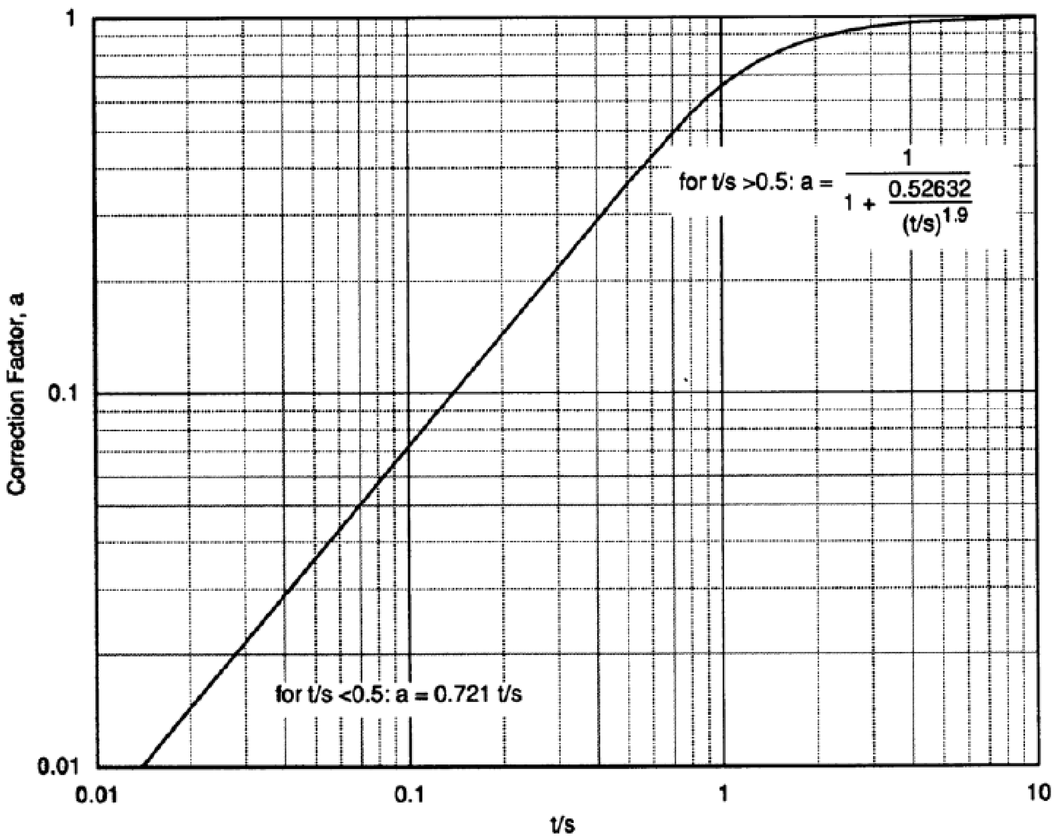

APPENDIX C

JCPDS-ICDD PDF Card No. 0014-6200

Sample Name	:	Tin (II) Sulfide
Crystal System	:	Orthorhombic
Lattice Type	:	*a* = 11.18 Å
		b = 3.98 Å
		c = 4.32 Å
Lattice Type	:	$\alpha = 90^0$
		$\gamma = 90^0$
		$\beta = 90^0$
Radiation	:	Cu $K_{\alpha 1}$
Wavelength	:	1.54 Å
2θ	:	10^0 - 80^0
Main Peaks	:	

(hkl)	D (Å)	2θ (^{0})
(111)	2.84075	31.47
(113)	2.108	42.846
(131)	2.311	38.924
(151)	1.786	51.092
(212)	1.455	63.903

APPENDIX D

Calculation of Crystallite Size (FWHM)

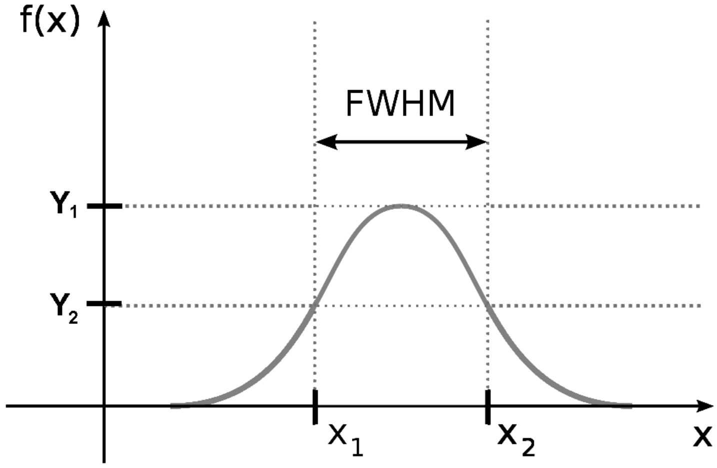

The value of full width half maximum for each graphs were calculated as follow,

$$FWHM = X_2 - X_1$$

The FWHM values for all samples are summarized in table below. All values obtained by using origin plot.

Sample Doping Concentration (wt%)	FWHM (rad)	
	As-deposited	Annealed
0	0.0098	0.0061
5	0.0089	0.0028
10	0.0053	0.0042
15	0.0066	0.0084
20	0.0115	0.0152

Crystallite Size Calculation for As-Deposited Samples

Scherrer's equation was utilized to calculate the crystallite size.

$$d = \frac{k\lambda}{\beta \cos\theta}$$

a) Crystallite size calculation for as-deposited SnS sample.

$$d = \frac{k\lambda}{\beta \cos\theta} = \frac{0.89(0.154056)}{0.0098 \cos 31.80} = 16nm$$

b) Crystallite size calculation for as-deposited 5 wt% Al;SnS sample.

$$d = \frac{k\lambda}{\beta \cos\theta} = \frac{0.89(0.154056)}{0.0089 \cos 31.75} = 18nm$$

c) Crystallite size calculation for as-deposited 10 wt% Al;SnS sample.

$$d = \frac{k\lambda}{\beta \cos\theta} = \frac{0.89(0.154056)}{0.0053 \cos 31.76} = 30nm$$

d) Crystallite size calculation for as-deposited 15 wt% Al;SnS sample.

$$d = \frac{k\lambda}{\beta \cos\theta} = \frac{0.89(0.154056)}{0.0066 \cos 31.86} = 24nm$$

e) Crystallite size calculation for as-deposited 20 wt% Al;SnS sample.

$$d = \frac{k\lambda}{\beta \cos\theta} = \frac{0.89(0.154056)}{0.0115 \cos 31.77} = 14nm$$

Crystallite size for all as-deposited samples.

Sample Doping Concentration (wt%)	Crystallite Size (nm)
0	16
5	18
10	30
15	24
20	14

Crystallite Size Calculation for Anneal Samples

Scherrer's equation was utilized to calculate the crystallite size.

$$d = \frac{k\lambda}{\beta \cos\theta}$$

a) Crystallite size calculation for anneal SnS sample.

$$d = \frac{k\lambda}{\beta \cos\theta} = \frac{0.89(0.154056)}{0.0061 \cos 31.90} = 26nm$$

b) Crystallite size calculation for anneal 5 wt% Al;SnS sample.

$$d = \frac{k\lambda}{\beta \cos\theta} = \frac{0.89(0.154056)}{0.0028 \cos 31.65} = 57nm$$

c) Crystallite size calculation for anneal 10 wt% Al;SnS sample.

$$d = \frac{k\lambda}{\beta \cos\theta} = \frac{0.89(0.154056)}{0.0042 \cos 31.75} = 38nm$$

d) Crystallite size calculation for anneal 15 wt% Al;SnS sample.

$$d = \frac{k\lambda}{\beta \cos\theta} = \frac{0.89(0.154056)}{0.0084 \cos 31.70} = 19nm$$

e) Crystallite size calculation for anneal 20 wt% Al;SnS sample.

$$d = \frac{k\lambda}{\beta \cos\theta} = \frac{0.89(0.154056)}{0.0152 \cos 31.75} = 11nm$$

Crystallite sizes for all anneal samples.

Sample Doping Concentration (wt%)	Crystallite Size (nm)
0	26
5	57
10	38
15	19
20	11

APPENDIX E

Calculation of Direct Band Gap for As-deposited Samples

a) Undoped tin (II) sulfide.

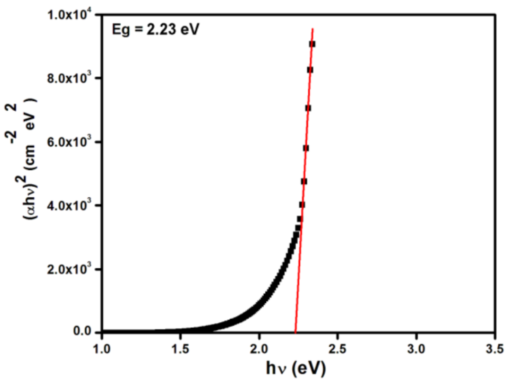

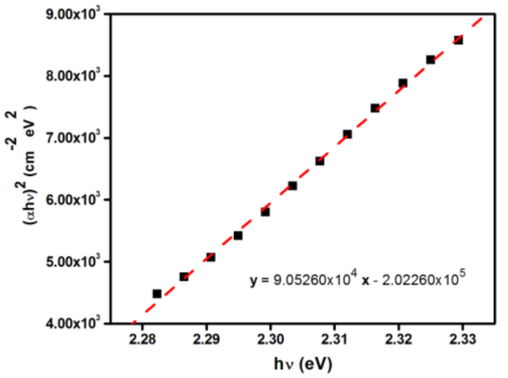

Linear fit equation for band gap calculation of as-deposited undoped tin (II) sulfide

When y = 0,

$$0 = 9.05260 \times 10^4 X - 2.02260 \times 10^5$$

$$X = \frac{2.02260 \times 10^5}{9.05260 \times 10^4}$$

$$X = 2.23eV$$

The value of direct band gap for as-deposited undoped tin (II) sulfide is 2.23 eV.

b) 5 wt% aluminum doped tin (II) sulfide.

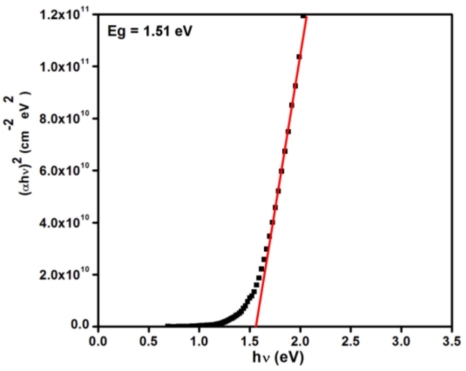

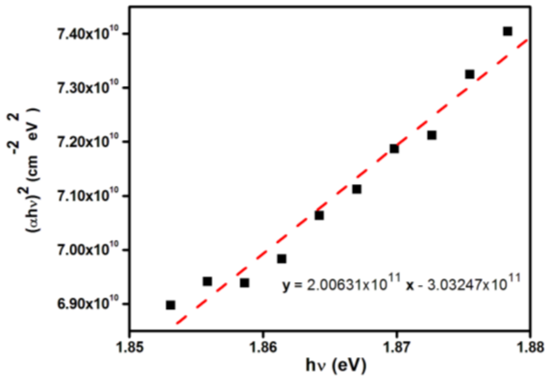

Linear fit equation for band gap calculation of as-deposited 5 wt% aluminum doped tin (II) sulfide.

When $y = 0$,

$$0 = 2.00631 \times 10^{11} X - 3.03247 \times 10^{11}$$

$$X = \frac{3.03247 \times 10^{11}}{2.00631 \times 10^{11}}$$

$$X = 1.51 eV$$

The value of direct band gap for as-deposited 5 wt% aluminum doped tin (II) sulfide is 1.51 eV.

c) 10 wt% aluminum doped tin (II) sulfide.

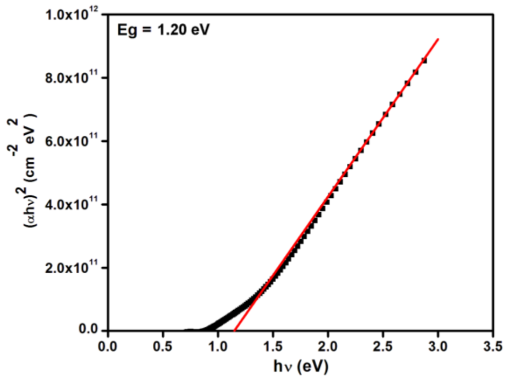

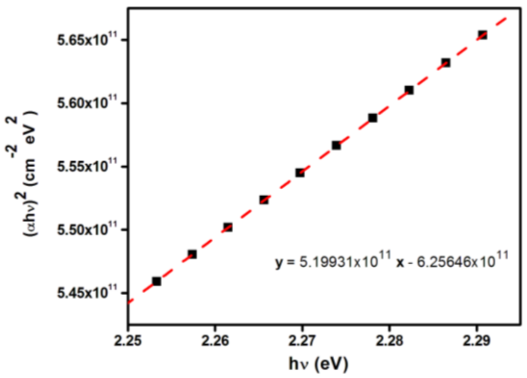

Linear fit equation for band gap calculation of as-deposited 10 wt% aluminum doped tin (II) sulfide.

When $y = 0$,

$$0 = 5.19931 \times 10^{11}X - 6.25646 \times 10^{11}$$

$$X = \frac{6.25646 \times 10^{11}}{5.19931 \times 10^{11}}$$

$$X = 1.20eV$$

The value of direct band gap for as-deposited 10 wt% aluminum doped tin (II) sulfide is 1.20 eV.

d) 15 wt% aluminum doped tin (II) sulfide.

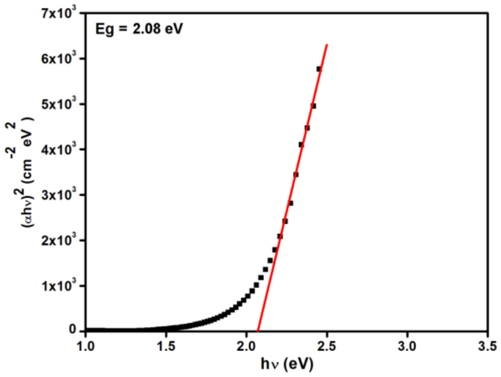

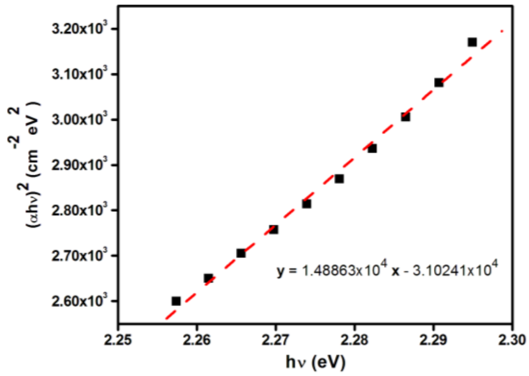

Linear fit equation for band gap calculation of as-deposited 15 wt% aluminum doped tin (II) sulfide.

When $y = 0$,

$$0 = 1.48863 \times 10^4 X - 3.10241 \times 10^4$$

$$X = \frac{3.10241 \times 10^4}{1.48863 \times 10^4}$$

$$X = 2.08eV$$

The value of direct band gap for as-deposited 15 wt% aluminum doped tin (II) sulfide is 2.08 eV.

e) 20 wt% aluminum doped tin (II) sulfide.

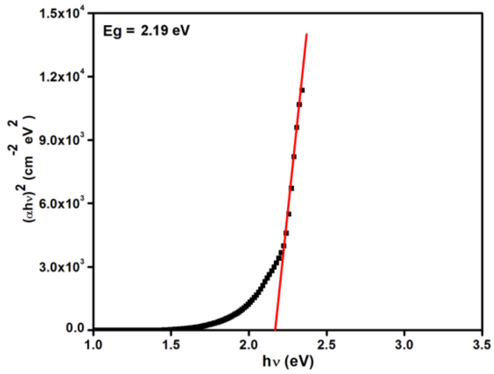

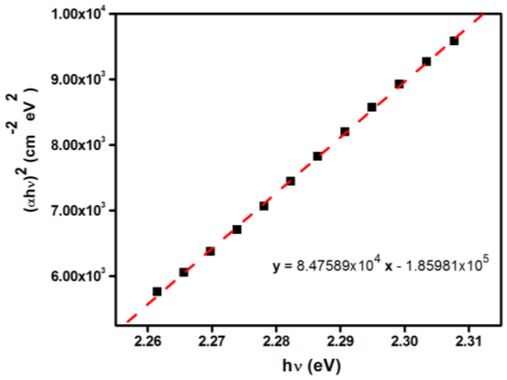

Linear fit equation for band gap calculation of As-deposited 20 wt% aluminum doped tin (II) sulfide.

At $y = 0$,

$$0 = 8.47589 \times 10^4 X - 1.85981 \times 10^5$$

$$X = \frac{1.85981 \times 10^5}{8.47589 \times 10^4}$$

$$X = 2.19eV$$

The value of direct band gap for as-deposited 20 wt% aluminum doped tin (II) sulfide is 2.19 eV.

APPENDIX F

Calculation of Direct Band Gap for Annealed Samples

a) undoped tin (II) sulfide.

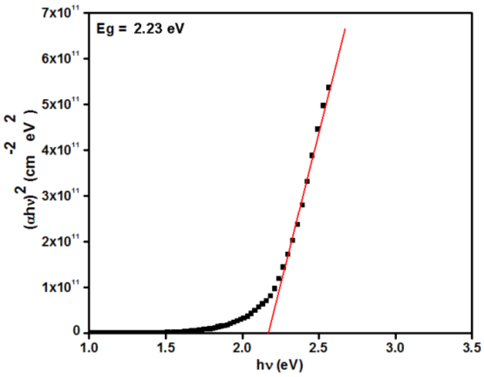

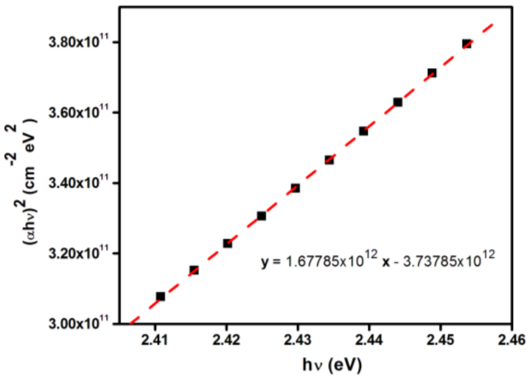

Linear fit equation for band gap calculation of annealed undoped tin (II) sulfide.

At $y = 0$,

$$0 = 1.67785 \times 10^{12} X - 3.73785 \times 10^{12}$$

$$X = \frac{3.73785 \times 10^{12}}{1.67785 \times 10^{12}}$$

$$X = 2.23eV$$

The value of direct band gap for annealed undoped tin (II) sulfide can be written as 2.23±0.01eV.

b) 5 wt% aluminum doped tin (II) sulfide.

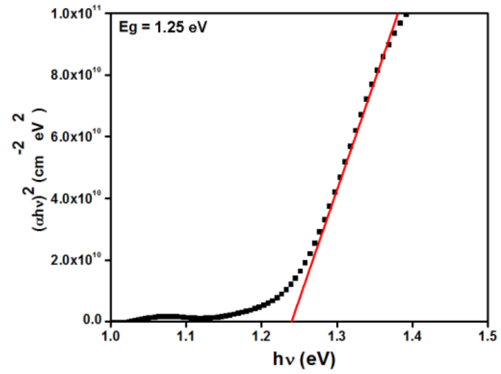

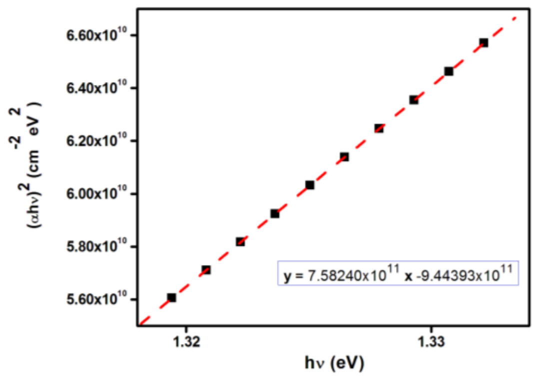

Linear fit equation for band gap calculation of Annealed 5 wt% aluminum doped tin (II) sulfide.

At $y = 0$,

$$0 = 7.58240 \times 10^{11}X - 9.44393 \times 10^{11}$$

$$X = \frac{9.44393 \times 10^{11}}{7.58240 \times 10^{11}}$$

$$X = 1.25eV$$

The value of direct band gap for annealed 5 wt% aluminum doped tin (II) sulfide is 1.25 eV.

c) 10 wt% aluminum doped tin (II) sulfide.

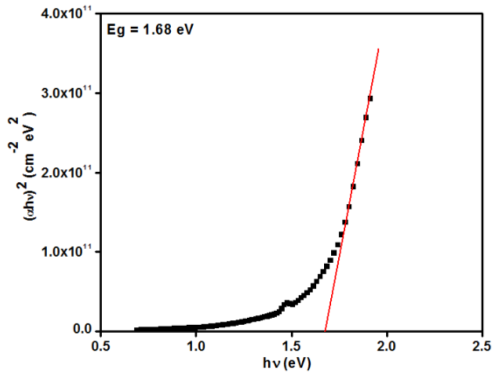

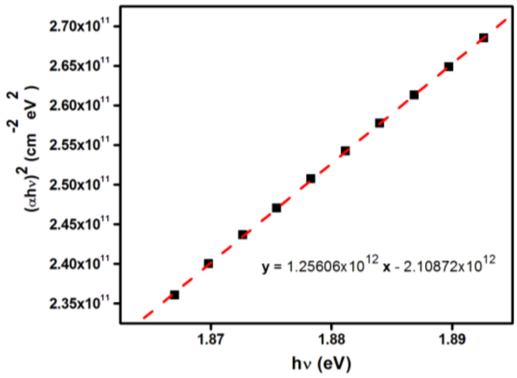

Linear fit equation for direct band gap calculation of Annealed 10 wt% aluminum doped tin (II) sulfide.

At $y = 0$,

$$0 = 1.25606 \times 10^{12}X - 2.10872 \times 10^{12}$$

$$X = \frac{2.10872 \times 10^{12}}{1.25606 \times 10^{12}}$$

$$X = 1.68eV$$

The value of direct band gap for annealed 10 wt% aluminum doped tin (II) sulfide is 1.68 eV.

d) 15 wt% aluminum doped tin (II) sulfide.

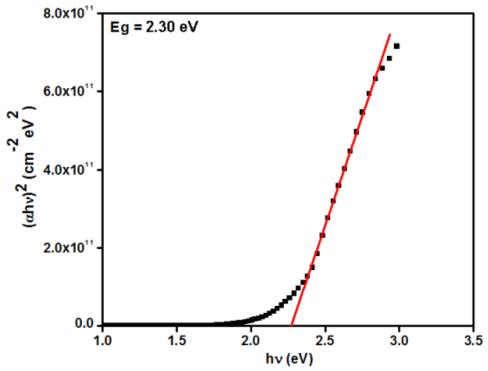

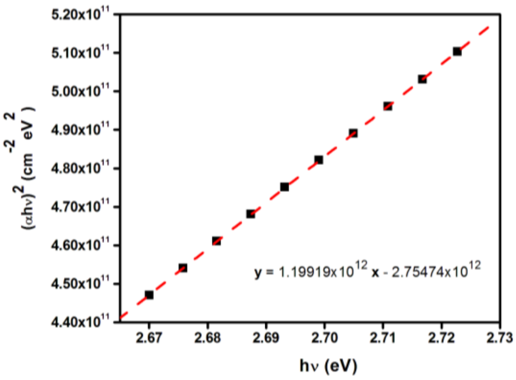

Linear fit equation for direct band gap calculation of Annealed 15wt% aluminum doped tin (II) sulfide.

At $y = 0$,

$$0 = 1.19919 \times 10^{12} X - 2.75474 \times 10^{12}$$

$$X = \frac{2.75474 \times 10^{12}}{1.19919 \times 10^{12}}$$

$$X = 2.30 eV$$

The value of direct band gap for annealed 15 wt% aluminum doped tin (II) sulfide is 2.30 eV.

e) 20 wt% aluminum doped tin (II) sulfide.

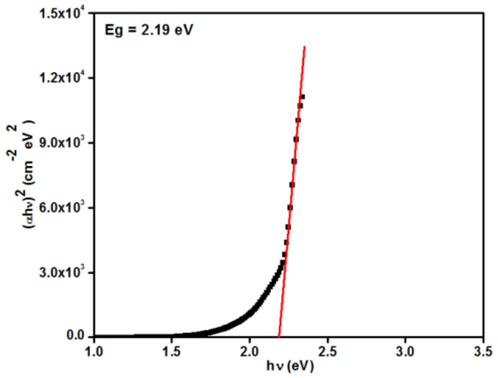

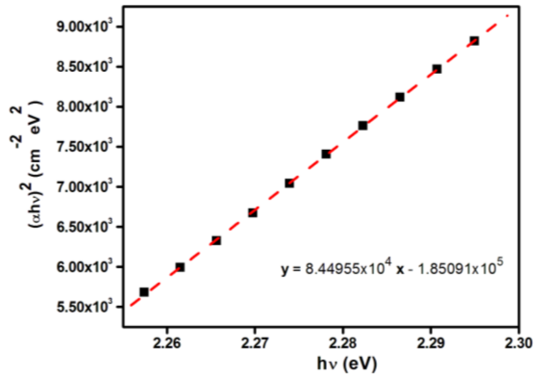

Linear fit equation for band gap calculation of Annealed 20 wt% aluminum doped tin (II) sulfide.

At $y = 0$,

$$0 = 8.44955 \times 10^4 X - 1.85091 \times 10^5$$

$$X = \frac{1.85091 \times 10^5}{8.44955 \times 10^4}$$

$$X = 2.19 eV$$

The value of direct band gap for annealed 20 wt% aluminum doped tin (II) sulfide is 2.19 eV.

APPENDIX G

Electrical Conductivity Calculation for As-Deposited Samples

It is given that, conductivity is $\sigma = \frac{1}{\rho}$

a) Conductivity calculation for as-deposited SnS sample.

$$\sigma = \frac{1}{\rho} = \frac{1}{22.879} = 0.044\ \Omega^{-1}m^{-1}$$

b) Conductivity calculation for as-deposited 5 wt% Al:SnS sample.

$$\sigma = \frac{1}{\rho} = \frac{1}{15.452} = 0.065\ \Omega^{-1}m^{-1}$$

c) Conductivity calculation for as-deposited 10 wt% Al:SnS sample.

$$\sigma = \frac{1}{\rho} = \frac{1}{0.009} = 111.111\ \Omega^{-1}m^{-1}$$

d) Conductivity calculation for as-deposited 15 wt% Al:SnS sample.

$$\sigma = \frac{1}{\rho} = \frac{1}{0.307} = 3.257\ \Omega^{-1}m^{-1}$$

e) Conductivity calculation for as-deposited 20 wt% Al:SnS sample.

$$\sigma = \frac{1}{\rho} = \frac{1}{3.892} = 0.257\ \Omega^{-1}m^{-1}$$

APPENDIX H

Absorption Coefficient Calculation for absorption coefficient (α) vs photon energy (hν) graph

It is given that, absorption coefficient is $\alpha = \frac{2.303A}{d}$

Where, A = Absorbance

D = Thickness of the samples (m)

Example;

$$\alpha = \frac{2.303A}{d} \quad = \frac{2.303(1.3227)}{400 \times 10^{-9}} \quad = 7615445.25$$

* All absorbance data are calculated in Microsoft Excel and plotted on absorption coefficient (α) vs photon energy (hν) graph.